



HAL
open science

Influence of pulsatile blood flow on allometry of aortic wall shear stress

G Croizat, A Kehren, H Roux de Bézieux, A. Barakat

► **To cite this version:**

G Croizat, A Kehren, H Roux de Bézieux, A. Barakat. Influence of pulsatile blood flow on allometry of aortic wall shear stress. 2018. hal-02410685

HAL Id: hal-02410685

<https://hal.science/hal-02410685>

Preprint submitted on 13 Dec 2019

HAL is a multi-disciplinary open access archive for the deposit and dissemination of scientific research documents, whether they are published or not. The documents may come from teaching and research institutions in France or abroad, or from public or private research centers.

L'archive ouverte pluridisciplinaire **HAL**, est destinée au dépôt et à la diffusion de documents scientifiques de niveau recherche, publiés ou non, émanant des établissements d'enseignement et de recherche français ou étrangers, des laboratoires publics ou privés.

Influence of pulsatile blood flow on allometry of aortic wall shear stress

G. Croizat, A. Kehren, H. Roux de Bézieux, A. Barakat

Laboratoire d'hydrodynamique de l'Ecole polytechnique (LADHYX)

9 Boulevard des Marchaux, 91120 Palaiseau, France

Abstract

Shear stress plays an important role in the creation and evolution of atherosclerosis. A key element for in-vivo measurements and extrapolations is the dependence of shear stress on body mass. In the case of a Poiseuille modeling of the blood flow, P. Weinberg and C. Ethier [2] have shown that shear stress on the aortic endothelium varied like body mass to the power $-\frac{3}{8}$, and was therefore 20-fold higher in mice than in men. However, by considering a more physiological oscillating Poiseuille - Womersley combined flow in the aorta, we show that results differ notably: at larger masses ($M > 10 \text{ kg}$) shear stress varies as body mass to the power $-\frac{1}{8}$ and modifies the man to mouse ratio to 1:8. The allometry and value of temporal gradient of shear stress also change: $\partial\tau/\partial t$ varies as $M^{-3/8}$ instead of $M^{-5/8}$ at larger masses, and the 1:150 ratio from man to mouse becomes 1:61. Lastly, we show that the unsteady component of blood flow does not influence the constant allometry of peak velocity on body mass: $u_{max} \propto M^0$. This work extends our knowledge on the dependence of hemodynamic parameters on body mass and paves the way for a more precise extrapolation of in-vivo measurements to humans and bigger mammals.

Introduction

The formation of atherosclerosis in arteries is a multifactorial process, still not fully understood in its mechanical factors ([12], ch. 23, p. 502). Yet, it has been shown that wall shear stress plays a key part in this phenomenon [1]. For theoretical analyses as well as for experimentation, it is very useful to know the dependence of wall shear stress τ in arteries, and especially in the aorta, on body mass M . It has long been assumed that wall shear stress was uniform across species, thus independent of body mass. However, recent works have shown that this assumption was not correct: allometric relationships, expressed as $\tau \sim M^\alpha$, with $\alpha \in \mathbb{R}$, can be obtained from simple models of blood flow in the aorta. Note that \propto shall be understood as "is proportional to". P. Weinberg and C. Ethier have modeled blood in the aorta as a Poiseuille flow and have deduced the following result: $\tau_{Poiseuille} \sim M^{-3/8}$ [2]. This result implies that wall shear stress in mice should be 20 times higher than in men. The objective of this article is to study the allometric relationship between body mass and wall shear stress and other key parameters with a more precise model of blood flow in the aorta. In order to be closer to physiology, we added a purely oscillatory unsteady profile to the steady Poiseuille one. This oscillating component is called Womersley flow.

We will first detail the mathematical derivation of the Poiseuille and Womersley profiles, before exploring their influence on the allometry of wall shear stress (WSS), temporal gradient of wall shear stress (TGWSS) and peak velocity.

1 Mathematical modeling

In everything that follows, blood is considered as an incompressible Newtonian fluid of density $\rho = 1060 \text{ kg.m}^{-3}$ and dynamic viscosity $\mu = 3.0 \cdot 10^{-3} \text{ Pa.s}$. The arteries are assumed to be rigid of radius a , and we adopt a no-slip condition on the arterial wall ($u(r = a) = 0$). We also assume the flow to be axisymmetric. Model-dependent hypotheses are described in the relevant subsections. See table 5 at the end of the document of all constants used in this work. All numeric simulations were done in Matlab R2016 a, The MathWorks, Inc., Natick, Massachusetts, United States. \log stands for logarithm in base 10, and \ln for natural logarithm.

1.1 Poiseuille flow

In the case of a Poiseuille flow, shear stress on the wall is worth:

$$\tau = 2\mu \frac{u_{max}}{a} \quad (1)$$

Let us detail the allometric arguments of equation 1, applied to the aortic artery:

- the aortic diameter a is assumed to vary as $M^{0.375}$, both from theoretical ([5]) and experimental considerations ([3] and [4])
- the dynamic viscosity of blood μ is assumed to be independent of the body mass
- the aortic velocity u_{max} can be seen as the cardiac flow rate divided the aortic cross-section $u_{max} = \frac{Q}{\pi a^2}$. The cardiac flow rate varies with $M^{0.75}$, as described in [5] and [6]. Therefore, u_{max} **is independent of M** .

We can conclude that in the case of a Poiseuille flow, wall shear stress scales as:

$$\tau_{Poiseuille} \propto M^{-0.375} \quad (2)$$

Additionally, we can deduce the allometry of temporal gradient of wall shear stress. Since $\frac{\partial \tau}{\partial t} \sim \omega \tau$, $\omega \sim M^{-0.25}$ being the cardiac frequency, we get:

$$\frac{\partial \tau}{\partial t}_{Poiseuille} \sim M_b^{-0.625} \quad (3)$$

We obtain the following values for mice, rabbits and humans (tab. 1), as described in [2], relatively to the human value:

Animal	Mass	Shear stress	Gradient of shear stress	Peak velocity
Human	75 kg	1	1	1
Rabbit	3.5 kg	3.0	6.8	1
Mouse	25 g	20.2	148.8	1

Table 1: Relative flow characteristics for various species - Poiseuille flow

1.2 Womersley flow

We consider a purely oscillating pressure gradient (eq. 5) in the same geometry, and derive the allometry of wall shear stress, temporal gradient of wall shear stress and peak velocity associated to this flow.

1.2.1 Ruling equations

In this context, the Navier-Stokes equation projected on z can be written as:

$$\rho \frac{\partial u}{\partial t} = -\nabla P + \mu \Delta u \quad (4)$$

We inject the expression of the pressure gradient (with $G_1 \in \mathbb{R}$ constant) in 4:

$$-\nabla P = \Re(G_1 \exp(i\omega t)) \quad (5)$$

as well as the expression of the velocity (note that $A(r) \in \mathbb{C}$):

$$u(r, t) = \Re(A(r) \exp(i\omega t)) \quad (6)$$

We obtain the following equation, ' being the differentiation with respect to r .

$$A'' + \frac{1}{r}A' - \frac{i\omega\rho}{\mu}A = -\frac{G_1}{\mu} \quad (7)$$

where we recognize the sum of a constant particular solution and a Bessel differential equation. We get the following velocity field, with J_0 the 0-order Bessel function of first kind. We also introduce the Womersley number $\alpha = a\sqrt{\frac{\omega\rho}{\mu}}$. This dimensionless number corresponds to the ratio of inertial transient forces to viscous forces.

$$u(r, t) = \Re\left(\frac{G_1}{i\omega\rho}\left(1 - \frac{J_0(i^{\frac{3}{2}}\alpha\frac{r}{a})}{J_0(i^{\frac{3}{2}}\alpha)}\right)e^{i\omega t}\right) \text{ on } \vec{u}_z \quad (8)$$

1.2.2 Derivation

Let us now calculate the flow rate Q :

$$Q(t) = \int_0^a u(r)2\pi r dr \quad (9)$$

and the wall shear stress τ :

$$\tau(t) = -\mu\frac{\partial u}{\partial r}\Big|_{r=a} \quad (10)$$

The calculation of (10) goes down to

$$\frac{\partial}{\partial r}[J_0(i^{\frac{3}{2}}\alpha\frac{r}{a})]\Big|_{r=a} \quad (11)$$

Using $J_0' = J_1$ in \mathbb{C} , we can conclude that

$$\tau(t) = \Re\left(\frac{aG_1}{i^{\frac{3}{2}}\alpha}\frac{J_1(\alpha i^{\frac{3}{2}})}{J_0(\alpha i^{\frac{3}{2}})}e^{i\omega t}\right) \quad (12)$$

Concerning (9), the key point is

$$\int_0^a rJ_0(i^{\frac{3}{2}}\alpha\frac{r}{a})dr \quad (13)$$

Using $x^n J_{n-1}(x) = \frac{d}{dx}(x^n J_n(x))$ for n in \mathbb{N}^* and x in \mathbb{C} , we get

$$Q(t) = \Re\left(\frac{\pi a^2 i G_1}{\omega\rho}\left(1 - \frac{2J_1(\alpha i^{\frac{3}{2}})}{\alpha i^{\frac{3}{2}} J_0(\alpha i^{\frac{3}{2}})}\right)e^{i\omega t}\right) \quad (14)$$

1.3 Physiological pulse wave: Poiseuille + Womersley flow

In reality, the pressure gradient is neither steady, nor purely oscillatory. It was shown ([13], [14]) that the pressure gradient ∇P could be reasonably approximated by the first six harmonics of its Fourier decomposition. In our case, six harmonics are not needed, as we are only looking at allometric variations. Along with the allometry of the Womersley flow (first harmonic), we will present the sum of Poiseuille and Womersley flows (fundamental + first harmonic), **which we denote PW flow from here on:**

$$u_{PW} = u_{Poiseuille} + u_{Womersley} \quad (15)$$

Consequently, by linearity of differentiation, wall shear stress and its temporal gradient are obtained by: $\tau_{PW} = \tau_{Poiseuille} + \tau_{Womersley}$ and $\nabla\tau_{PW} = \nabla\tau_{Poiseuille} + \nabla\tau_{Womersley}$. Concerning peak velocity however, calculations are done using the total velocity field u_{PW} .

2 Results

2.1 Wall shear stress (WSS)

To evaluate the allometry of wall shear stress, we need to know the allometry of every variable present in its expression. Concerning a , α or ω , the allometry is known from [2], as summed up in table 5. But the allometry of G_1 is unknown. To overcome this problem, we substitute the flow rate Q , which follows an experimentally determined allometry $Q \sim M^{0.75}$. This step can be discussed, since the Womersley flow model implies a zero average flow rate. Although $\langle Q \rangle$, the time average value of Q , is always null, its effective value $\langle Q^2 \rangle$ is indeed an increasing function of body mass, which justifies the use of $Q \propto M^{0.75}$ in the Womersley model. Combining (12) and (14), we obtain

$$\underline{\tau} = \frac{\omega \rho J_1(x)}{\pi a i (x J_0(x) - 2 J_1(x))} \underline{Q} \quad (16)$$

with $x = i^{\frac{3}{2}} \alpha$ and \underline{Q} , $\underline{\tau}$ the complex variables such that $Q = \Re(\underline{Q})$ and $\tau = \Re(\underline{\tau})$.

We introduce the following function f , such that $\underline{\tau} = \frac{\omega \rho}{\pi a} f(\alpha) \underline{Q}$:

$$f(\alpha) = \frac{i J_1(x)}{(2 J_1(x) - x J_0(x))} \quad (17)$$

We plot $|\Re(f)|$ as a function of α in logarithmic scale on figure 1). Note that $\Re(f)$ is negative, ie $|\Re(f)| = -\Re(f)$.

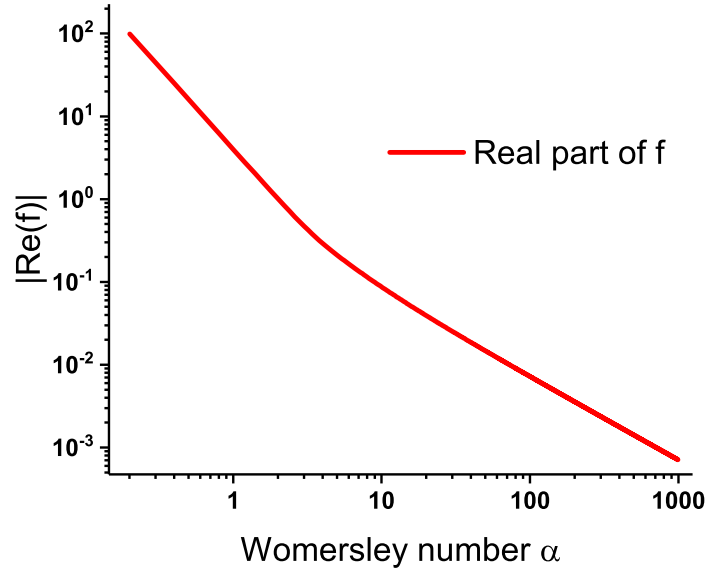


Figure 1: Graph of $\log|\Re(f)|$ as a function of α , logarithmic scale. We can clearly identify two power laws: $\Re(f) \propto \alpha^{-2}$ for $\alpha < 2$, and $\Re(f) \propto \alpha^{-1}$ for $\alpha > 5$

- for $\alpha < 2$, $\Re(f) \sim \alpha^{-2}$ ($r^2 = 0.98$)
- for $\alpha > 5$, $\Re(f) \sim \alpha^{-1}$ ($r^2 = 0.99$)

We can confirm these regressions using Taylor and asymptotic developments of J_0 and J_1 :

$$J_0(x) = 1 - x^2/4 + O_0(x^4) \quad (18)$$

and

$$J_1(x) = x/2 - x^3/16 + O_0(x^5) \quad (19)$$

using big O notation ([16], p. 687).

Consequently, for $\alpha \ll 1$, $f(\alpha) \approx 4i/x^2 \approx -4/\alpha^2$, which confirms $\Re(f) \sim \alpha^{-2}$ for $\alpha \ll 1$.

Conversely, for $|x| \rightarrow +\infty$:

$$J_0(x) \approx \sqrt{\frac{2}{\pi x}} \cos(x - \pi/4) \quad (20)$$

and

$$J_1(x) \approx \sqrt{\frac{2}{\pi x}} \sin(x - \pi/4) \quad (21)$$

introducing complex sine and cosine ([16], p. 723).

In our case, $x = i^{3/2}\alpha = \alpha \exp(3i\pi/4)$, therefore $f(\alpha) \approx -\frac{i \tan(x)}{x} = \frac{\tanh(\alpha\sqrt{2}/2)}{\alpha} \exp(-3i\pi/4)$ and finally $\Re(f(\alpha)) \approx \frac{\sqrt{2}}{2\alpha}$, which confirms $\Re(f) \sim \alpha^{-1}$ for $\alpha \rightarrow \infty$.

Knowing that $\alpha \sim M^{0.25}$, and that $\frac{\omega\rho Q}{\pi a} \sim M^{0.125}$ (see table 5 at the end of the document), we obtain:

$$\boxed{\tau_{womersley} \sim M^{-0.375} \text{ for } M < 1 \text{ kg}} \text{ and } \boxed{\tau_{womersley} \sim M^{-0.125} \text{ for } M > 10 \text{ kg}}$$

which differs notably from

$$\boxed{\tau_{poiseuille} \sim M^{-0.375} \text{ for all } M}$$

We can complete the previous chart of relative shear stress for different animals (tab. 2).

We also plot the compared shear stress induced by a Poiseuille, Womersley or physiological PW flows as a function

Animal	Mass	α_{aorta}	Shear stress (Poiseuille)	Shear stress (Womersley)	Shear stress (PW)
Human	75 kg	13	1	1	1
Rabbit	3.5 kg	6	3.0	1.7	1.8
Mouse	25 g	1.8	20.2	7.6	8.2

Table 2: Relative shear stress for various species - Poiseuille, Womersley, and Poiseuille + Womersley (PW) flows

of mass on figure 2. First of all, we can see that despite several allometric approximations (flow rate, heart rate, aortic radius, Womersley number), the absolute value of wall shear stress $\tau \in [0.1; 10] \text{ Pa}$ is within the range of measured values ([12], ch. , p.502). We observe that Poiseuille shear stress is, in absolute value, much lower than Womersley stress (10 to 20 times lower as mass increases). At low masses ($M < 1 \text{ kg}$), both flows follow the same allometry: $\tau_{PW} \propto M^{-0.375}$. At higher masses however, ($M > 10 \text{ kg}$), the Womersley stress accounts for the variations of total stress and thus $\tau_{PW} \propto M^{-0.125}$. In practice, it means that **the difference in wall shear stress between mice and men is greatly reduced by the influence of pulsatile flow in larger arteries**, and shows the necessity of the unsteady modeling of blood flow for correct body mass allometries.

2.2 Temporal gradient of wall shear stress (TGWSS)

Concerning the temporal gradient of shear stress, we get $\frac{\partial \tau}{\partial t} \sim \omega \tau$, with $\omega \sim M^{-0.25}$ [2], and therefore:

$$\boxed{\frac{\partial \tau}{\partial t}_{wom} \sim M_b^{-0.625} \text{ for } M < 1 \text{ kg}} \text{ and } \boxed{\frac{\partial \tau}{\partial t}_{wom} \sim M_b^{-0.375} \text{ for } M > 10 \text{ kg}}$$

Which should be compared to

$$\boxed{\frac{\partial \tau}{\partial t}_{poi} \sim M^{-0.625} \text{ for all } M}$$

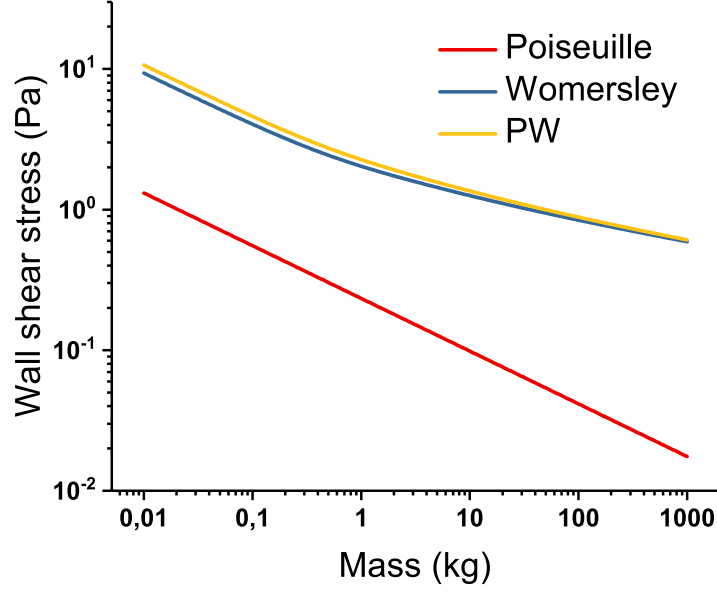


Figure 2: Compared wall shear stresses for Poiseuille, Womersley and PW flows as a function of body mass - logarithmic scale. We observe that Poiseuille stress is globally dominated, in absolute value, by Womersley stress: Poiseuille makes only 12% of total stress for a mouse ($M = 0.025 \text{ kg}$), and this percentage goes down to 5% for a human ($M = 75 \text{ kg}$). Concerning allometry, both processes induce $\tau_{PW} \propto M^{-0.375}$ at low masses ($M < 1 \text{ kg}$), but at higher masses ($M > 10 \text{ kg}$), the Womersley stress sets the allometry $\tau_{PW} \propto M^{-0.125}$.

We compare the values of shear stress gradient between Womersley and Poiseuille in tab. 3. Poiseuille TGWSS is lower than Womersley TGWSS, and the allometric domination at high masses is also present. The graph of these functions (fig. 3) is very similar to the one on wall shear stress (fig. 2). At low masses ($M < 1 \text{ kg}$), both flows result in $\frac{\partial \tau}{\partial t} PW \propto M^{-0.625}$ allometry, and at higher masses ($M > 10 \text{ kg}$), Womersley stresses dominate the allometry: $\frac{\partial \tau}{\partial t} PW \propto M^{-0.375}$. Here again, we observe a reduced difference between men and mice due to the influence of unsteady flow at high Womersley numbers.

Animal	Shear stress gradient (Poiseuille)	Shear stress gradient (Womersley)	Shear stress gradient (PW)
Human	1	1	1
Rabbit	6.8	3.8	3.9
Mouse	148.8	55.8	60.5

Table 3: Relative shear stress for various species - Poiseuille vs Womersley flow

2.3 Peak velocity

And finally, we can express the maximum velocity. First we inject the expression of the flow rate in the Womersley velocity to absorb the time dependence (again using $x = i^{3/2}\alpha$):

$$u_{Wom}(r) = \frac{Q}{\pi a^2} \times \frac{J_0(xr/a) - J_0(x)}{xJ_0(x) - 2J_1(x)} \quad (22)$$

We know that $\frac{Q}{\pi a^2}$ is independent of α (table 5), therefore

$$u_{max}^{Wom}(\alpha) \propto \max_{r \in [0, a]} \Re \left(\frac{J_0(xr/a) - J_0(x)}{xJ_0(x) - 2J_1(x)} \right) = \max_{r \in [0, a]} (g_{wom}(\alpha)) \quad (23)$$

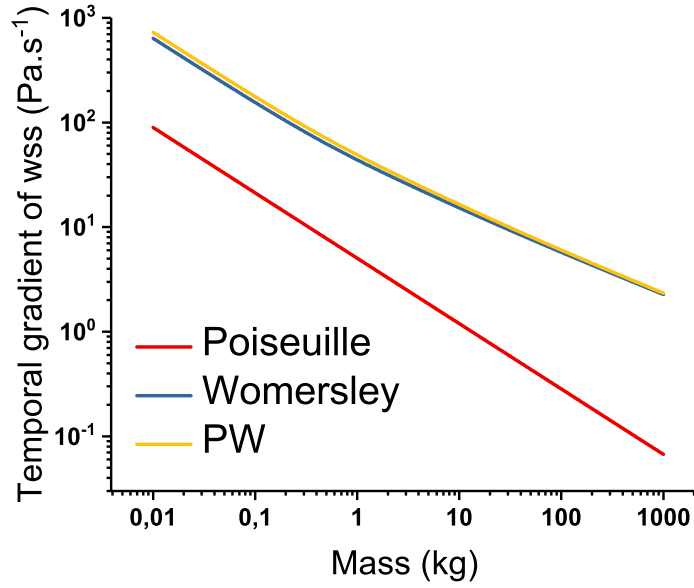


Figure 3: Compared temporal gradient of wall shear stresses for Poiseuille, Womersley and PW flows as a function of body mass - logarithmic scale. Poiseuille TGWSS is much smaller than Womersley TGWSS. At low masses ($M < 1kg$), $\frac{\partial \tau}{\partial t} PW \propto M^{-0.625}$, while at higher masses ($M > 10kg$), the Womersley stress accounts for the body mass allometry $\frac{\partial \tau}{\partial t} PW \propto M^{-0.375}$.

Recalling equivalents of J_0 and J_1 (eq. 18 to 21), we can find equivalents of $g_{wom}(\alpha)$ at low and high α :

- for $M \ll 1$, $g_{wom} \sim \frac{\sqrt{2}}{2\alpha} \sim M^{-0.25}$, we observe a divergence:

$$\lim_{M \rightarrow 0} u_{max}^{Wom} = +\infty$$

- for $M \gg 1$, we also obtain $g_{wom} \sim \frac{1}{\alpha} \sim M^{-0.25}$, and

$$\lim_{M \rightarrow +\infty} u_{max}^{Wom} = 0$$

We plot $\max_r(g_{wom})$, which represents the Womersley peak velocity only, as a function of M on figure 4. We also add the Poiseuille peak velocity.

Concerning PW flow, calculations must be done considering the total velocity field: recalling the expression of u_{Poiss} as a function of Q and r : $u_{Poiss} = \frac{2Q}{\pi a^2}(1 - \frac{r}{a})$, u_{max}^{PW} is:

$$u_{max}^{PW}(\alpha) \propto \max_{r \in [0, a]} \Re \left(2\left(1 - \frac{r}{a}\right) + \frac{J_0(xr/a) - J_0(x)}{xJ_0(x) - 2J_1(x)} \right) = \max_{r \in [0, a]} (g_{PW}(\alpha)) \quad (24)$$

On figure 4, we can see that the Womersley flow alone gives rise to a peak velocity which vanishes with M (blue curve), while the PW flow (yellow curve) shows a constant peak velocity for reasonably high M . This proves that the constant peak velocity measured experimentally [18] is due to the steady Poiseuille component of the flow, rather than to the Womersley unsteady component. We also observe that the maximum velocity is systematically reached in the center of the artery ($r = 0$, data not shown), which is not the case for a pure Womersley flow at high Womersley number. This confirms the domination of the Poiseuille flow. Figure 4 further proves the necessity of a combined Poiseuille - Womersley flow to account for the variations of the different hemodynamic parameters.

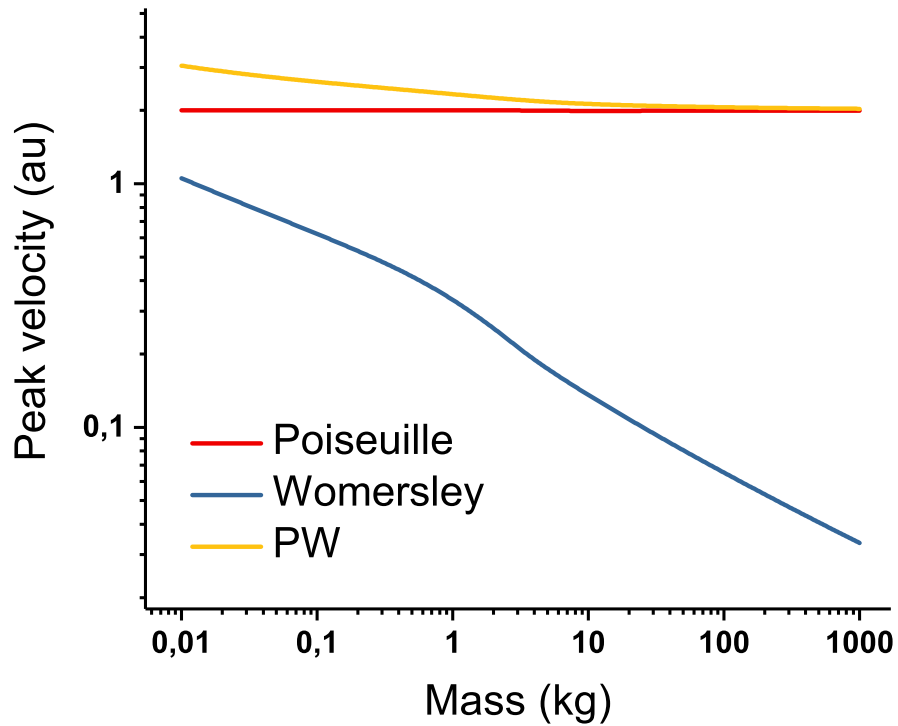


Figure 4: Peak velocity of Poiseuille, Womersley and PW flows as a function of mass, logarithmic scales: the constant peak velocity observed experimentally ([18]) is due to the Poiseuille component rather than the Womersley one which vanishes at high M

2.4 Summary of the different allometric laws

We summarize the different allometries obtained throughout this work in table 4.

Flow modeling	Poiseuille	Womersley		PW	
		$M < 1 \text{ kg}$	$M > 10 \text{ kg}$	$M < 1 \text{ kg}$	$M > 10 \text{ kg}$
Hemodynamic parameter					
WSS	-0.375	-0.375	-0.125	-0.375	-0.125
TGWSS	-0.625	-0.625	-0.375	-0.625	-0.375
Peak velocity	0	-0.25		0	

Table 4: Summary of body mass allometry of different hemodynamic parameters

Conclusion

In this study, we have recalled the derivation of wall shear stress, temporal gradient of wall shear stress and peak velocity, for a Poiseuille and subsequently Womersley modeling of the blood flow in the aorta. We have shown that a Poiseuille modeling alone (and equivalently, a Womersley modeling alone) was not able to account for the variations of the previously mentioned parameters. We showed that a combination of Poiseuille and Womersley flows, here called PW flow, was necessary to conduct an allometry study.

- Concerning wall shear stress, Poiseuille and Womersley flows agree on a $M^{-0.375}$ at low Womersley numbers, while the Womersley component dominates at higher α ($M^{-0.125}$ against $M^{-0.375}$). This changes the

”Twenty-fold difference in hemodynamic wall shear stress between murine and human aortas” advanced in [2] to a lower 8.2 fold difference.

- About the temporal gradient of wall shear stress, the same phenomenon occurs: while $M^{-0.625}$ is valid at low α , the unsteady component dominates at higher α ($M^{-0.375}$ against $M^{-0.625}$), and brings mice to men ratio from 150 : 1 to 61 : 1.
- For peak velocity on the contrary, the independance on α observed experimentally [18] is due to the Poiseuille component rather than to the Womersley one, which follows a vanishing $u_{max}^{wom} \propto M^{-0.25}$.

As a consequence, only considering a Poiseuille flow to infer the wall shear stress allometry in mammals is not a precise method. On the contrary, one should take into account the two components of the blood flow profile (steady Poiseuille and unsteady Womersley), to account for their respective ranges of domination. This work gives a new insight on the allometry of 3 key hemodynamic parameters in atherosclerosis. It can also help extrapolate measurements from small mammals like mice, which are common in cardiovascular laboratories, to bigger ones and to humans. A comprehensive imaging study of aortic velocity profiles on heavy mammals could help support or reject this theory and greatly benefit the field.

Appendix

Physical quantity	Body mass allometry	Human value ($M = 75 \text{ kg}$)	Scaling constant (IS unit)
Aortic radius	$a_0 M^{0.375}$	1.5 cm	$a_0 = 3.0 \cdot 10^{-3} \text{ m}$
Flow rate	$Q_0 M^{0.75}$	5L/min = $8.3 \cdot 10^{-5} \text{ m}^3/\text{s}$	$Q_0 = 3.3 \cdot 10^{-6} \text{ m}^3 \cdot \text{s}^{-1}$
Cardiac pulsation ($2\pi \cdot$ frequency)	$w_0 M^{-0.25}$	$7.35 \text{ rad} \cdot \text{s}^{-1} = 70 \text{ bpm}$	$w_0 = 21.6 \text{ rad} \cdot \text{s}^{-1}$
Womersley number	$\alpha_0 M^{0.25}$	13	$\alpha_0 = 4.4$
Blood dynamic viscosity	μM^0	/	$\mu = 3.0 \cdot 10^{-3} \text{ Pa} \cdot \text{s}$
Blood density	ρM^0	/	$\rho = 1.06 \cdot 10^3 \text{ kg} \cdot \text{m}^{-3}$

Table 5: Body mass allometry of different body parameters. The scaling constants were determined to match the value of the human proximal aorta

References

- [1] Cunningham KS., Gotlieb AI., *The role of shear stress in the pathogenesis of atherosclerosis* Lab Invest. 2005 Jul;85(7):942
- [2] P. Weinberg, C. Ethier, *Twenty-fold difference in hemodynamic wall shear stress between murine and human aortas*. Journal of Biomechanics 40, 2007
- [3] Clark, A.J., *Comparative physiology of the heart* MacMillan, New-York, 1927
- [4] Holt, J.P., Rhode, E.A., Holt, W.W., Kines, H. *Geometric similarities of aortas, venae cavae and certain of their branches in mammals* American Journal of Physiology Regulatory, Integrative and Comparative Physiology 241, 1981
- [5] West, G.B., Brown, J.H., Enquist, B.J.. *A general model for the origin of allometric scaling laws in biology* Science 276, 1997
- [6] Kleiber, M., *Body size and metabolism* Hilgardia 6, 315-353, 1932

- [7] Castier, Y., Brandes, R.P., Leseche, G., Tedgui, A., Lehoux, S. 2005 *p47phox-dependent NADPH oxidase regulates ow-induced vascular remodeling* Circulation Research 97, 533-540, 2005
- [8] Ibrahim, J., Miyashiro, J.K., Berk, B.C., *Shear stress is differentially regulated among inbred rat strains* Circulation Research 92, 10011009, 2003
- [9] Lacy, J.L., Nanavaty, T., Dai, D., Nayak, N., Haynes, N., Martin, C., *Development and validation of a novel technique for murine rst-pass radionuclide angiography with a fast multiwire camera and tantalum 178* Journal of Nuclear Cardiology 8, 171181, 2001
- [10] Khir, A.W., Henein, M.Y., Koh, T., Das, S.K., Parker, K.H., Gibson, D.G., *Arterial waves in humans during peripheral vascular surgery* Clinical Science (London) 101, 749757, 2001
- [11] J. Mestel *Pulsatile flow in a long straight artery* Lecture 14, Biofluid Mechanics, Imperial College, 2009
- [12] W. Nichols, M. O'Rourke, C. Vlachopoulos, A. Hoeks, R. Reneman - *McDonald's blod flow in arteries - Sixth edition - Chapter 10 - Contours of pressure and flow waves in arteries*
- [13] Tracy Morland - *Gravitational Effects On Blood Flow* - Mathematical Biology group, University of Colorado at Boulder, available at mathbio.colorado.edu/index.php/MBW:Gravitational_Effects_on_Blood_Flow
- [14] J.R. Womersley - *Method for the calculation of velocity, rate of flow and viscous drag in arteries when the pressure gradient is known* - Journal of Physiology (1955) 127, p. 553-563
- [15] C. Cheng & al. - *Review: Large variations in wall shear stress levels within one species and between species* - Atherosclerosis, December 2007, Volume 195, Issue 2, Pages 225235
- [16] G. Arfken, H. Weber - *Mathematical methods for physicists, sixth edition* - Elsevier Acedemic Press, 2005
- [17] J. Greve & al. - *Allometric Scaling of Wall Shear Stress from Mouse to Man: Quantification Using Cine Phase-Contrast MRI and Computational Fluid Dynamics* - American Journal of Physiology - Heart and Circulatory Physiology, May 19, 2006
- [18] K. Schmidt-Nielsen - *Scaling Why is Animal Size so Important?* - Cambridge University Press, Cambridge 1984
- [19] Greve et al. *Allometric scaling of wall shear stress from mice to humans quantification using cine phase-contrast MRI and computational uid dynamics* Am. J. Physiol. Heart. Circ. Physiol. 291, 2006

